Appl. Phys. B 82, 65–70 (2006)
DOI: 10.1007/s00340-005-2042-8

Applied Physics B
Lasers and Optics

G. QIN✉
S. HUANG
Y. FENG
A. SHIRAKAWA
M. MUSHA
K.-I. UEDA

Power scaling of Tm^{3+} doped ZBLAN blue upconversion fiber lasers: modeling and experiments

Institute for Laser Science, University of Electro-communications,
1-5-1 Chofugaoka, Tokyo 182-8585, Japan

Received: 11 June 2005/Revised version: 25 August 2005
Published online: 4 November 2005 • © Springer-Verlag 2005

ABSTRACT Power scaling of Tm^{3+} doped ZBLAN blue upconversion fiber lasers was investigated by a simple model. Based on our experimental results on blue fiber lasers, we discuss the effects of photodegradation and photocuring, fiber length, the reflectivity of the coupler mirror and fiber core diameter on further enhancement of blue fiber laser, respectively. The optimal parameters (including fiber length, fiber core diameter and the reflectivity of the coupler mirror) for the operation of high power (> 1 W) blue fiber laser were presented through simple numerical simulations, which are valuable for the future design of high power blue upconversion fiber laser.

PACS 42.55.Wd; 42.60. Lh

1 Introduction

In recent years, rare earth ions doped upconversion fiber lasers have attracted much attention due to a wide range of applications including high-density optical data storage, all color displays, undersea communications and biomedicine. Up to now, room-temperature visible upconversion fluoride glass (doped with Tm^{3+}, Pr^{3+}, Er^{3+}, Ho^{3+} and Yb^{3+}) fiber lasers have been obtained [1–12]. Paschotta et al. [4] reported a 230 mW blue upconversion laser in Tm^{3+} doped ZrF_4-BaF_2-LaF_3-AlF_3-NaF (ZBLAN) glass fiber. Zellmer and co-workers [10, 11] demonstrated red, green and blue upconversion lasers in Pr^{3+} and Yb^{3+} co-doped ZBLAN fibers. At present, high-power (> 1 W) visible, and especially blue, upconversion fiber lasers are the next objective for the researchers. Among the above-mentioned fluoride fiber lasers, the efficiency of blue lasers in Tm^{3+} doped ZBLAN fiber is the highest by as much as 31.7%. Though the existence of the photodegradation effect in Tm^{3+} doped ZBLAN fiber at high pump power limits the output power of blue fiber lasers to several hundred mW level [13–16], it is believed that high power blue fiber laser can be obtained with the improvement of the ZBLAN fiber material (through the modulation of the composition of fluoride fiber, the introducing of other ions into the core of ZBLAN fiber to preclude the photodegradation effect, etc.).

✉ Fax: +81-424-85-8960, E-mail: gsqin@yahoo.com

For the construction of blue fiber lasers, some numerical simulations based on a theoretical model is necessary for the understanding and further optimization of the device. In this case, Duclos et al. [17] presented a model of Tm^{3+} doped ZBLAN blue upconversion fiber laser. Paschotta and co-workers [18] calculated optimized parameters for such lasers through the characterization of the upconversion spectra in this fiber. Both cases were limited to low power operation (< 1 W) of blue upconversion fiber laser. As mentioned above, high power blue fiber lasers can be realized with the development of the ZBLAN fiber material. In this paper, power scaling of Tm^{3+} doped ZBLAN blue upconversion fiber lasers was investigated by a simple model, which is similar to that reported by Paschotta [18]. Based on our experimental results on blue fiber lasers, we discussed the effects of photodegradation and photocuring, fiber length, the reflectivity of the coupler mirror and fiber core diameter on further enhancement of blue fiber laser, respectively. The optimal parameters (including fiber length, fiber core diameter and the reflectivity of the coupler mirror) for the operation of high power (> 1 W) blue fiber laser were presented through simple numerical simulations, which is valuable for the future design of high power blue upconversion fiber laser.

2 Modeling of Tm^{3+} doped ZBLAN blue upconversion fiber lasers

The upconversion mechanism in Tm^{3+} doped fluoride glass fiber excited at 1120 nm has been investigated widely, as shown in Fig. 1. First, by excitation with an 1120 nm laser, the electrons at the ground state are promoted to the $^3H_5$ level. Through multiphonon nonradiative relaxation they populate the $^3F_4$ level, then the $^3F_3$ level, the $^3H_4$ level and the state $^1G_4$. In Fig. 1, we define simplified labels 1 to 6 for the levels that we subsequently use in this paper. The excited-state populations of Tm^{3+} in ZBLAN glass fiber at a particular pump power can be described by rate equations, assuming purely homogeneous broadening of the levels. Note that in this paper, we fix the concentration of Tm^{3+} at 1000 ppm due to the unexpected effects (including stronger photodegradation effect, energy transfer between pairs of ions, etc.) caused by high doping concentration of Tm^{3+} in ZBLAN glass fiber, which are very harmful for the enhancement of blue fiber laser power. We started with the

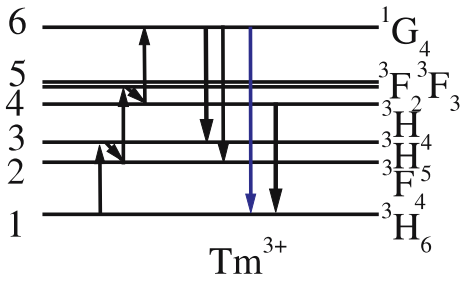

FIGURE 1 The upconversion mechanism in Tm^{3+} doped fluoride glass fiber excited at 1120 nm

following simplified version without considering the terms for energy transfer between pairs of ions due to low doping concentration of Tm^{3+} (~ 1000 ppm):

$$\frac{dn_1}{dt} = -(R_{13} + W_{16})n_1 + A_{21}n_2 + A_{41}n_4 + (A_{61} + W_{16})n_6 , \quad (1)$$

$$\frac{dn_2}{dt} = R_{13}n_1 - R_{25}n_2 - A_{21}n_2 + A_{42}n_4 + (A_{62} + A_{63})n_6 , \quad (2)$$

$$\frac{dn_4}{dt} = R_{25}n_2 - R_{46}n_4 + n_{64}n_6 + (A_{64} + A_{65})n_6 - A_4n_4 , \quad (3)$$

$$\frac{dn_6}{dt} = W_{16}n_1 + R_{46}n_4 - R_{64}n_6 - A_6n_6 - W_{61}n_6 , \quad (4)$$

$$n_3 \approx 0, n_5 \approx 0, n_1 + n_2 + n_4 + n_6 \approx 1 , \quad (5)$$

where the notation n_j (a number between 0 and 1) represents the fraction of ions in level j, the terms R_{13}, R_{25}, R_{46}, and R_{64} pump rates given, e.g., by

$$R_{13} = \sigma_{13}\frac{I_p}{h\nu_p} , \quad (6)$$

(σ_{13} is the absorption cross section for the first pump transition and I_p the pump intensity in Watt per square meter), $W_{i,j}$ the signal transition rates, the A coefficients radiative decays, e.g., A_{21} for the decay from level 2 to level 1, and the total decay rates are $A_6 = \sum_j A_{6j}$ and $A_4 = \sum_j A_{4j}$. In (5), we used the fact that the levels 3 and 5 decay very rapidly by multiphonon nonradiative relaxation to the levels immediately below. In addition, a consequence of treating the multiphonon decay of levels 3 and 5 as instantaneous is that the corresponding pump rates appear directly in the rate equations of the lower levels.

The laser oscillator model is based on powers rather than complex field components, and so it does not account for longitudinal modes or phenomena such as spatial hole burning. Amplified spontaneous emission (ASE) is not included in the laser oscillator model. The bi-directional propagation equations for the signal are stated as

$$\frac{dS^{\pm}}{d(zn_t\sigma_{61})} = \pm\left(n_6 - \frac{\sigma_{16}}{\sigma_{61}}n_1\right)S^{\pm} \mp \alpha_s S^{\pm}/(n_t\sigma_{61}) . \quad (7)$$

(Here, a rectangle wave model for the waveguide modes in Tm^{3+} doped ZBLAN glass fiber is assumed for simplicity without the reduction of the accuracy. α_s is the background loss of the signal, n_t the total population intensity)

TABLE 1 The parameters for the numerical simulations

Cross-section values (10^{-27} m^2)	A Coefficient values (s^{-1})
$\sigma_{16} = 16$	$A_{21} = 152$
$\sigma_{61} = 122$	$A_{41} = 665$
$\sigma_{64} = 69$	$A_{42} = 55$
$\sigma_{13} = 92$	$A_{61} = 600$
$\sigma_{25} = 60$	$A_{62} = 100$
$\sigma_{46} = 180$	$A_{63} = 430$
	$A_{64} = 138$
	$A_{65} = 36$

Equations (7) are coupled, and they conform to a simple relationship derived from the product rule of differentiation: $S^+S^- = C$, where C is a constant. Thus (7) can be decoupled by use of the cavity boundary conditions, which are

$$S^+(z=0) = R_1S^-(z=0),\ R_2S^+(z=z_{end}) = S^-(z=z_{end}) . \quad (8)$$

[where z_{end} is the cavity length, R_1 the reflectivity at 480 nm of the mirror 1 (high transmission at 1120 nm and high reflectivity at 480 nm), R_2 the reflectivity at 480 nm of the coupler mirror 2 (high transmission at 1120 nm)]

For the pump wave, we assume that it makes a single transit from $z = 0$ in the forward (+) direction:

$$\frac{dI_p}{d(zn_t\sigma_{61})} = -\left(\frac{\sigma_{13}}{\sigma_{61}}n_1 + \frac{\sigma_{25}}{\sigma_{61}}n_2 + \frac{\sigma_{46}}{\sigma_{61}}n_4 - \frac{\sigma_{64}}{\sigma_{61}}n_6\right)I_p - \alpha_p I_p/(n_t\sigma_{61}) . \quad (9)$$

[where α_p is the background loss of the pump wave.]

Table 1 shows the parameters for the numerical simulations, which are obtained from [18]. Equations (1)–(9) are solved numerically with Matlab software, and the solutions will be presented in the following sections.

3 Experimental results on blue upconversion fiber laser

In our experiments the pump laser was a Raman fiber laser operating at 1120 nm or 1140 nm, pumped by a 1064 nm (or 1100 nm) Yb^{3+}-doped fiber laser, which is similar to a previous report on a 1178 nm Raman fiber laser [19]. The commercial Tm-doped ZBLAN fluoride fiber (LeVerre Fluore, France) that we used had a thulium concentration of 1000 ppm (by weight), a numerical aperture of 0.19, and a core diameter of 3 μm, corresponding to a cutoff wavelength of 800 nm. The background loss at 480 nm of this fiber was about 0.07 dB/m. Both fiber ends were cut by a FK-11 fiber cleaver with the tension of 50–60 g, and the measurement results by a microscope showed that the cleaved surfaces were very flat. We launched an 1120 nm (or 1140 nm) pump light into the fiber core through a couple of aspheric lenses. Tests with a short fluoride fiber (10 cm) showed that the launched efficiency, defined as the launched power divided by the power incident on the lens, was about 60%. For the mirrors forming the cavity, one has a high reflectivity ($\sim 99.9\%$) at 480 nm and a high transmission at 1120 nm, and the other has 80% (or 60%) reflectivity at 480 nm and a high transmission at 1120 nm. Both mirrors were butted directly with

the fiber end. The output spectrum of the fiber end and the launched or output power were measured using an AQ-6315A optical spectrum analyzer (ANDO, Japan) and a LABMASTER optical power meter (Coherent, USA), respectively.

Using a 1.8-m ZBLAN fiber as the gain medium, a blue upconversion fiber laser can be obtained with an 80% or a 60% reflectivity mirror, respectively. Figure 2a shows the spectrum of a blue upconversion fiber laser with the linewidth of less than 0.05 nm (the resolution limit of the AQ-6315A optical spectrum analyzer). The output power of this blue laser was measured, as shown in Fig. 2b. As we can see from Fig. 2b, for the output mirror with 80% reflectivity, the slop efficiency is about 15%, the optical-to-optical conversion efficiency of 11%, and its maximum unsaturated output power is 116 mW. When we replaced the 80% reflectivity output mirror with 60% reflectivity, repeated measurements show that the slop efficiency is about 18% and the optical-to-optical conversion efficiency is 12%, but its maximum saturated output power is about 80 mW. To verify that this was not related to the deterioration of the fiber end, we put back the 80% reflectivity mirror without recleaving the fiber and reproduced the results obtained previously with that mirror. The experimental result was the same as that in Fig. 2b, which showed that the fiber end was not deteriorated by the high power blue laser.

To understand why blue fiber laser with the 60% reflectivity output mirror presents saturated output power but that with the 80% reflectivity output mirror not, we make some numerical simulations on this laser. For the initial simulations, the launched pump power is fixed at 1 W, the background loss of ZBLAN glass fiber was obtained as much as 0.7 dB/m through simulations with the data of the 80% reflectivity output mirror, as shown in Fig. 2b, which is higher than the measured value (~ 0.07 dB/m) due to the existence of the photodegradation effect in the operation of blue fiber laser. Using 0.7 dB/m as the value of the background loss, the dependence of blue fiber laser output power on the pump power were obtained for the cavity with different reflectivity output mirrors, as shown in Fig. 3a. As we can see from Fig. 3a, the cavity with 60% reflectivity output mirror shows higher output power and efficiency than that with 80% reflectivity [18]. As we all know, the cavity with larger background loss (e.g., ~ 2 dB at 480 nm) produces lower output power blue fiber laser at the same pump power. Based on our previous experimental results [20], a competition between photodegradation and photocuring in the operation of a blue fiber laser greatly affects the maximum output power of it [21]. That is to say, we consider that the intra-cavity intensity of the blue fiber laser with an 80% reflectivity mirror should be three times higher than that with a 60% reflectivity mirror at the same output power, such a higher intra-cavity blue laser can make the fiber core cure more efficiently (e.g., at the same pump power, the degradation effect may be nearly same for these two blue lasers. But for the cavity with an 80% reflectivity output mirror, the intra-cavity intensity of the blue laser is higher than that with a 60% reflectivity output mirror, the curing effect of the blue laser should be more efficient), and further allow higher output power of the blue laser in Tm^{3+} doped ZBLAN glass fiber. Figure 3b shows the dependence of the pump power, forward and back signals on the position in the fiber (here, the pump power is 1 W, and the background loss at 480 nm 0.7 dB/m), which shows that for 1 W pump power,

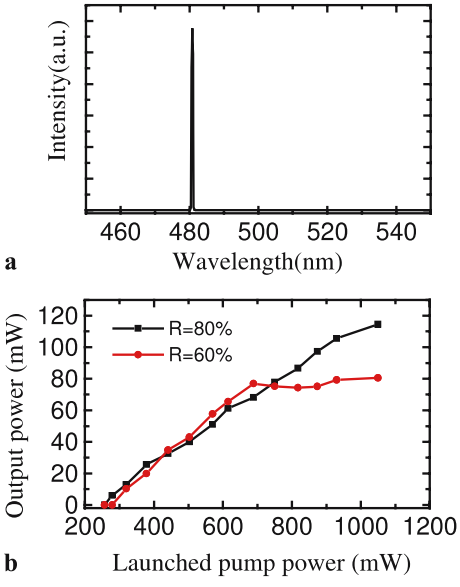

FIGURE 2 (**a**) Blue up conversion laser emission spectrum in 1.8 m ZBLAN glass fiber. (**b**) Measured output power of blue up conversion fiber laser with 80% or 60% reflectivity output mirror, respectively

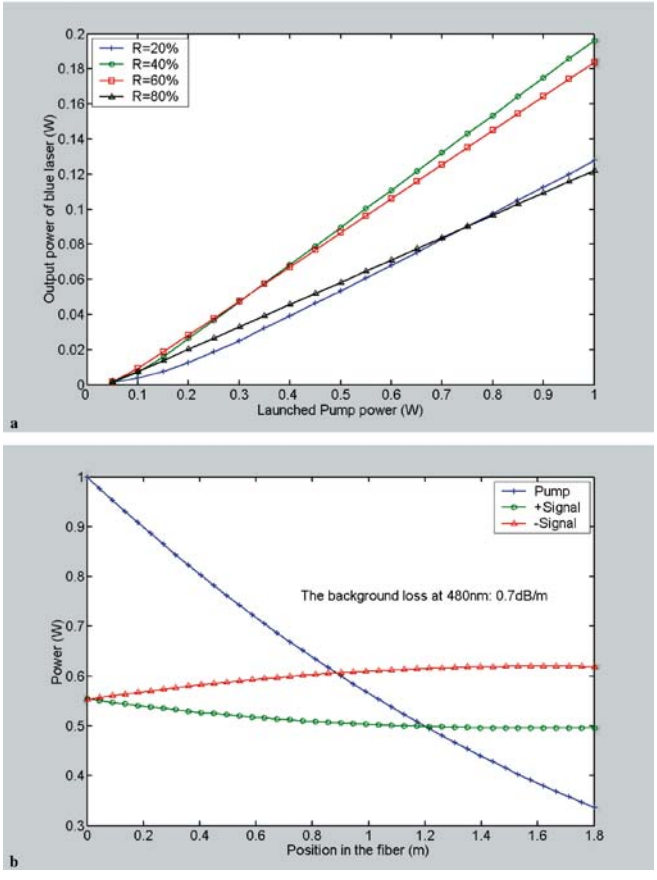

FIGURE 3 (**a**) The dependence of blue fiber laser output power on the pump power were obtained for the cavity with different reflectivity output mirrors. (**b**) The dependence of the pump power, forward and back signals on the position in the fiber (here, the pump power is 1 W, and the background loss at 480 nm 0.7 dB/m)

1.8 m fiber produces the maximum output power with the loss of 30% pump power. Though the cavity with high reflectivity at 1120 nm coupler mirror can enhance the output power and the efficiency, in this case, the back fiber end will be deteriorated easily by the high power blue laser and the back reflecting pump light. In addition, considering the loss of 30% pump power, the real efficiency should be higher than that shown in Fig. 2b.

We also carried out blue upconversion laser experiments with an 1140 nm Raman fiber laser as the pump source. Using a 2.5 m Tm^{3+} doped ZBLAN fiber as the gain medium, a 140 mW blue upconversion fiber laser can be obtained with an 80% reflectivity output mirror. Though 1140 nm laser pumped blue upconversion laser shows higher efficiency than 1120 nm laser pumped blue laser due to large absorption of ZBLAN:Tm^{3+} fiber to 1140 nm laser (larger than that of to 1120 nm laser), there is another problem for 1140 nm laser pumped blue laser, i.e., high power 1140 nm laser make ZBLAN:Tm^{3+} fiber burned easily at the natural bending point (at this moment, the output power of blue laser is only 140 mW). We think such burning may be due to large absorption of ZBLAN:Tm^{3+} fiber to 1140 nm laser. It should be noted that, for 1120 nm (or 1064 nm) laser pumped blue fiber laser, it is not a problem due to the relatively low absorption of the fiber to them.

In the operation of our blue upconversion fiber laser, we observed 784 nm ($^1G_4 \rightarrow {}^3H_5$ transition) amplified spontaneous emission signals (data not shown), which is detrimental for the operation of blue upconversion fiber laser (the detailed effects of 784 nm ASE on the blue up conversion fiber lasers has been discussed in [22]). We think that in future experiments both the input and the output mirrors should be made of high transmission at 784 nm by use of coating technology that can inhibit 784 nm lasing and further optimize blue upconversion fiber lasing.

Figure 4 describes the optimal parameters including fiber length, the reflectivity of the coupler mirror at 1 W pump power without considering the photodegradation and photocuring effects, which show that the cavity with low reflectivity output mirror produces the highest output power, the optimal reflectivity exists at a particular fiber length, the optimal reflectivity becomes lower and lower with increasing the fiber length, and the optimal fiber length exists at 1 W pump power.

Considering the above-mentioned experimental results, for the present commercial ZBLAN fiber, the cavity with the low reflectivity output mirror can not produce the optimal blue laser due to the existence of a competition between photodegradation and photocuring in the operation of a blue fiber laser [20, 21]. Though the existence of the photodegradation effect in Tm^{3+} doped ZBLAN fiber at high pump power limits the output power of blue fiber lasers to several hundred mW level, it is believed that high power blue fiber laser can be obtained with the improvement of the ZBLAN fiber material (through the modulation of the composition of fluoride fiber, the introducing of other ions into the core of ZBLAN fiber to preclude the photodegradation effect, etc.).

4 Power scaling of Tm^{3+} doped ZBLAN blue upconversion fiber lasers: numerical simulations

As mentioned above, high power blue fiber laser can be realized with the development of the ZBLAN fiber material. Considering the development history of high power Yb^{3+} doped fiber laser, large core fiber can allow larger output power. Large core fiber can also reduce the effect of the photodegradation phenomenon on the operation of high power blue upconversion fiber laser. In this section, we investigate power scaling (> 1 W) of blue upconversion fiber lasers with different core diameter varied from 3 μm to 20 μm through numerical simulations. In order to investigate the pure effects of the core diameter of the fiber on high power operation of blue fiber laser, the pump power is fixed at 10 W, the background loss at 480 nm 0.7 dB/m (in fact, larger core fiber has larger background loss. Here, the background loss of the fiber with the core diameter varied from 3 μm to 20 μm are fixed at

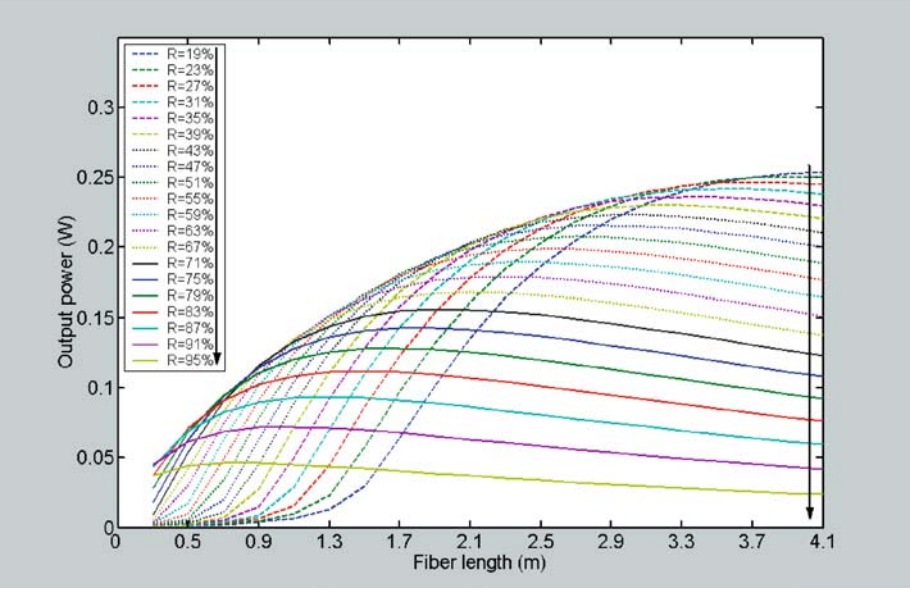

FIGURE 4 Simulated optimal parameters including fiber length, the reflectivity of the coupler mirror of blue laser cavity at 1 W pump power without considering the photodegradation and photocuring effects

the same value for studying the pure effects of the core diameter of the fiber on high power operation of blue fiber laser) the background loss at 1120 nm 0.1 dB/m, and the output mirror high transmission at 1120 nm. With these parameters and those presented in Table 1, (1)–(9) are solved numerically with Matlab software, and the optimal parameters including fiber length, fiber core diameter and the reflectivity of the coupler mirror for the operation of high power (> 1 W) blue fiber laser were obtained at 10 W pump power without considering the photodegradation and photocuring effects, as shown in Fig. 5. As we can see from Fig. 5, first, for the core diameter of 3 μm, 6 μm, 12 μm, 20 μm, the maximum output power of blue fiber lasers are 2.9 W, 2.83 W, 2.34 W, 1.76 W, respectively. Second, there exists an optimal output power point, including the optimal fiber length and the reflectivity of the output mirror at a particular core diameter, the maximum output power of the blue fiber laser decreases with an increasing core diameter of Tm^{3+} doped ZBLAN fiber; the optimal fiber length decreases with an increasing the core diameter of the fiber. In our numerical simulations, the background loss at 480 nm is fixed at 0.7 dB/m for the core diameter varied from 3 μm to 20 μm. In fact, larger core fiber has larger background loss, which will make the real output power lower than that described in Fig. 5.

Why does the maximum output power of blue fiber laser decrease with increasing the core diameter of the fiber? As we all know, blue upconversion luminescence is a three-photon absorption anti-stokes process, as shown in Fig. 1. Figure 6 shows the relations of the population of the states to the pump density at static state (no lasing). From Fig. 6, the ratio $\frac{n_6}{n_1+n_2+n_4+n_6}$ increases with increasing the pump density. In our experiments, blue upconversion luminescence is a three-photon absorption nonlinear process, and blue upconversion laser also a three-photon absorption nonlinear process. Though there is a different behavior in level population under lasing and non lasing conditions, the electrons are promoted from the ground state to the excited state step by step with the excitation of the pump laser for these two conditions. That is to say, the level population process is similar under lasing and non lasing conditions. As we can see from Fig. 6, with decreasing the pump density, more electrons are distributed into the states n_1, n_2 and n_4, which will reduce the efficiency of blue upconversion process and further the output power of blue upconversion laser. Considering the dependence of the maximum output power of blue fiber laser on the core diameter of the fiber, for the same pump power (10 W), larger core means lower pump density, which make more electrons distributed into the states n_1, n_2 and n_4, and further reduce the efficiency and output power of blue upconversion laser.

In addition, why does the optimal fiber length drop with a rising core diameter of the fiber? We consider that the optimal fiber length of the fiber laser depends on the pump distribution in the fiber. Generally, for a front-end pumped fiber laser, there exists a pump power distribution in the fiber, and

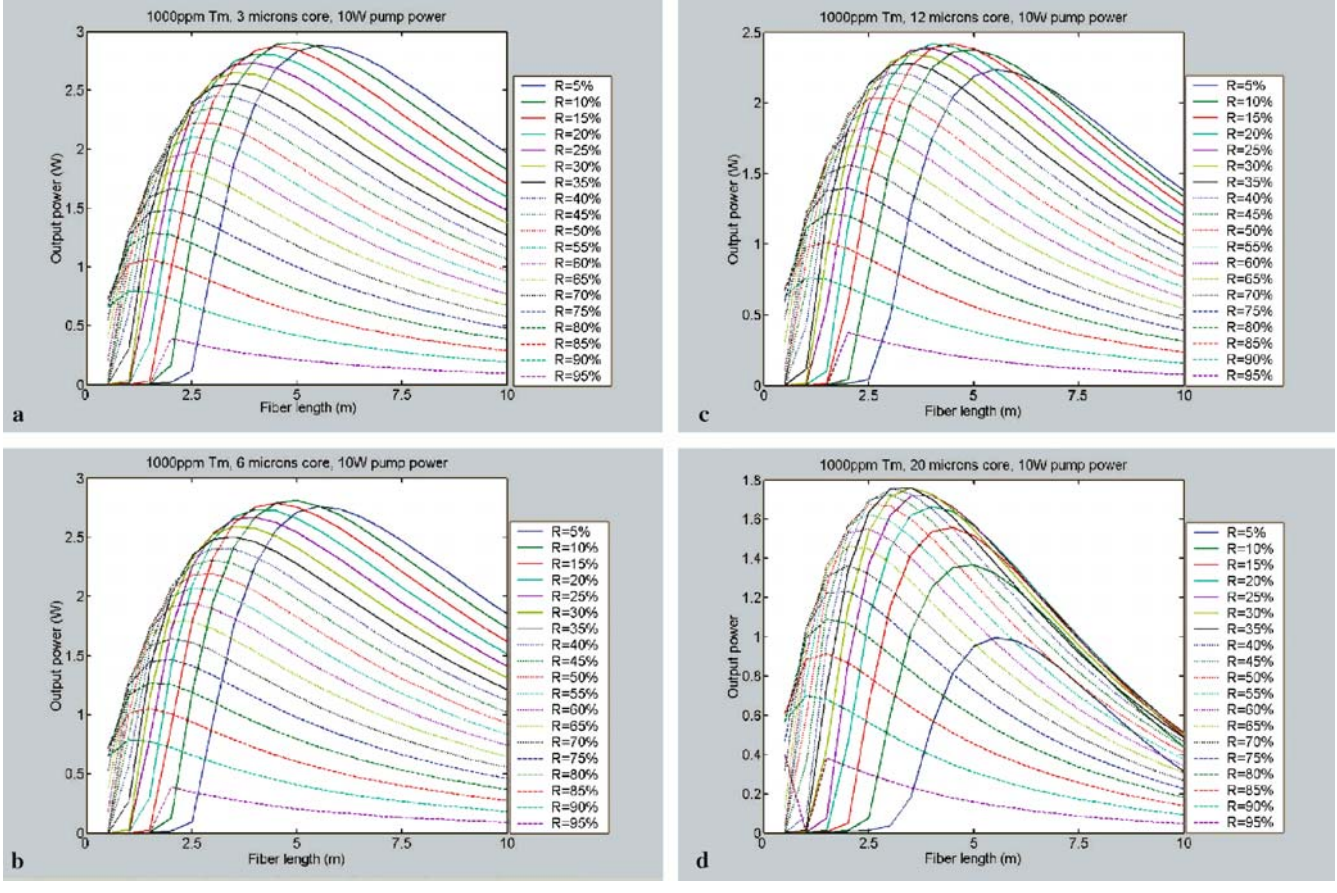

FIGURE 5 Simulated optimal parameters including fiber length, fiber core diameter and the reflectivity of the coupler mirror for the operation of high power (> 1 W) blue fiber laser at 10 W pump power without considering the photodegradation and photocuring effects

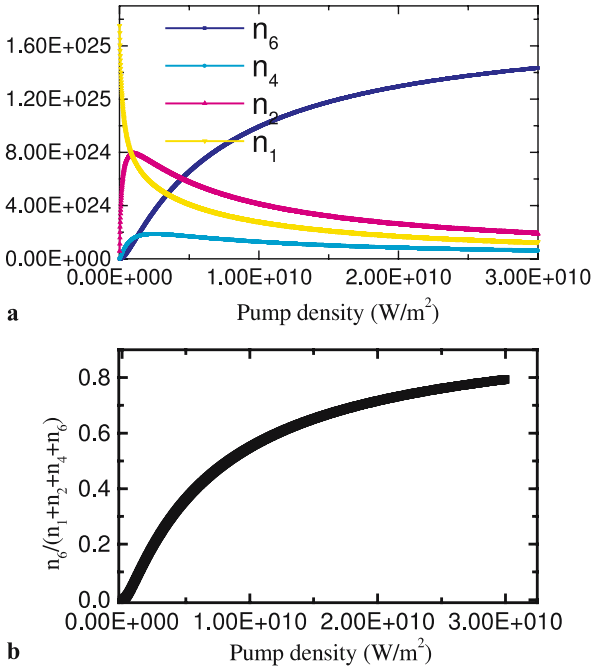

FIGURE 6 The relations of the population of the states to the pump density at static state (no lasing)

the front part of the fiber can be pumped efficiently. But if the fiber length is too long, the back part of the fiber will not be pumped efficiently, which will reduce the efficiency and the output power of the device. So there exists the optimal fiber length. In our experiments (front-end pumped way), at the same pump power, more pump power is distributed at the front part of fiber due to large absorption to the pump laser in large core fiber compared with that in small core fiber, which make the optimal fiber length become shorter for large core fiber than that for small core fiber. Therefore, the optimal fiber length drops with rising the core diameter.

5 Conclusion

Power scaling of Tm^{3+} doped ZBLAN blue upconversion fiber lasers was investigated by a simple model. Based on our experimental results on blue fiber lasers, the effects of photodegradation and photocuring, fiber length, the reflectivity of the coupler mirror and fiber core diameter on further enhancement of blue fiber laser were discussed, respectively. Though the existence of the photodegradation effect in Tm^{3+} doped ZBLAN fiber at high pump power limits the output power of blue fiber lasers to several hundred mW level, it is believed that high power blue fiber laser can be obtained with the improvement of the ZBLAN fiber material (through the modulation of the composition of fluoride fiber, the introducing of other ions into the core of ZBLAN fiber to preclude the photodegradation effect, etc.). The optimal parameters (including fiber length, fiber core diameter and the reflectivity of the coupler mirror) for the operation of high power (> 1 W) blue fiber laser were presented through simple numerical simulations, which is valuable for the future design of high power blue upconversion fiber laser.

ACKNOWLEDGEMENTS This work was partly supported by the 21st century COE Program of the Ministry of Education, Culture, Sports, Science and Technology of Japan.

REFERENCES

1 J.Y. Allain, M. Monerie, H. Poignant, Electron. Lett. **26**, 166 (1990)
2 S. Sanders, R.G. Waarts, D.G. Mehuys, D.F. Welch, Appl. Phys. Lett. **67**, 1815 (1995)
3 S.G. Grubb, K.W. Bennett, R.S. Cannon, W.F. Humer, Electron. Lett. **28**, 1243 (1992)
4 R. Paschotta, N. Moore, W.A. Clarkson, A.C. Tropper, D.C. Hanna, G. Maze, IEEE J. Sel. Top. Quantum Electron. **3**, 1100 (1997)
5 D.S. Funk, J.G. Eden, J.S. Osinski, B. Lu, Electron. Lett. **33**, 1958 (1997)
6 H.M. Pask, A.C. Tropper, D.C. Hanna, Opt. Comm. **134**, 139 (1997)
7 D.M. Baney, G. Rankin, K.W. Chang, Appl. Phys. Lett. **69**, 1662 (1996)
8 T. Sandrock, H. Scheife, E. Heumann, G. Huber, Opt. Lett. **22**, 808 (1997)
9 H. Zellmer, P. Riedel, A. Tunnermann, Appl. Phys. B. **69**, 417 (1999)
10 H. Zellmer, P. Riedel, M. Kempe, A. Tunnermann, Electron. Lett. **38**, 1250 (2002)
11 M. Zeller, H.G. Limberger, T. Lasser, IEEE Photon. Technol. Lett. **15**, 194 (2003)
12 I.J. Booth, C.J. Mackechine, B.F. Ventrudo, IEEE J. Quantum Electron. **32**, 118 (1996)
13 P.R. Barber, R. Paschotta, A.C. Tropper, D.C. Hanna, Opt. Lett. **20**, 2195 (1995)
14 P. Laperle, A. Chandonnet, R. Vall'ee, Opt. Lett. **20**, 2484 (1995)
15 I.J. Booth, J.-L. Archambault, B.F. Ventrudo, Opt. Lett. **21**, 348 (1996)
16 P. Laperle, A. Chandonnet, R. Vall'ee, Opt. Lett. **22**, 178 (1997)
17 F. Duclos, P. Urquhart, J. Opt. Soc. Am. B. **12**, 709 (1997)
18 R. Paschotta, P.R. Barber, A.C. Tropper, D.C. Hanna, G. Maze, J. Opt. Soc. Am. B. **14**, 1213 (1997)
19 S, Huang, Y. Feng, A. Shirakawa, K.-I Ueda, Jpn. J. Appl. Phys. **42**, L1439 (2003)
20 G. Qin, S. Huang, Y. Feng, A. Shirakawa, M. Musha, K.-I. Ueda, J. Appl. Phys. **97**, 126 108 (2005)
21 P. Laperle, R. Vall'ee, A. Chandonnet, Opt. Commun. **175**, 221 (2000)
22 G. Qin, S. Huang, Y. Feng, A. Shirakawa, K.-I. Ueda, Opt. Lett. **30**, 269 (2005)